AGU PUBLICATIONS

Journal of Advances in Modeling Earth Systems

RESEARCH ARTICLE

10.1002/2017MS001109

Key Points:

- Field observation experiment of surface solar spectral radiation
- The impact of solar elevation angle and soil moisture on the diurnal variation characteristics of bare soil surface albedo
- Solar elevation angle is a significant factor of controlling the diurnal variation characteristics of bare soil surface albedo

Supporting Information:

- Supporting Information S1

Correspondence to:
Z. Zheng,
zhiyzheng@outlook.com

Citation:
Zheng, Z., Wei, Z., Wen, Z., Dong, W., Li, Z., Wen, X., . . . Yan, D. (2017). Inclusion of solar elevation angle in land surface albedo parameterization over bare soil surface. *Journal of Advances in Modeling Earth Systems*, *9*, 3069–3081. https://doi.org/10.1002/2017MS001109

Received 30 JUN 2017
Accepted 30 OCT 2017
Accepted article online 7 DEC 2017
Published online 29 DEC 2017

Inclusion of Solar Elevation Angle in Land Surface Albedo Parameterization Over Bare Soil Surface

Zhiyuan Zheng[1,2,3], Zhigang Wei[1,2,4], Zhiping Wen[1], Wenjie Dong[1,4], Zhenchao Li[3], Xiaohang Wen[4,5], Xian Zhu[2,4], Dong Ji[2,4], Chen Chen[2,4], and Dongdong Yan[2,4]

[1]Center for Monsoon and Environment Research, Guangdong Province Key Laboratory for Climate Change and Natural Disaster Studies, School of Atmospheric Sciences, Sun Yat-Sen University, Guangzhou, China, [2]State Key Laboratory of Earth Surface Processes and Resource Ecology, Faculty of Geographical Science, Beijing Normal University, Beijing, China, [3]Key Laboratory of Land Surface Process and Climate Change in Cold and Arid Regions, Northwest Institute of Eco-Environment and Resources, Chinese Academy of Sciences, Lanzhou, China, [4]Zhuhai Joint Innovative Center for Climate-Environment-Ecosystem, Key Laboratory of Urban Climate and Ecodynamics, Future Earth Research Institute, Beijing Normal University, Zhuhai, China, [5]Plateau Atmosphere and Environment Key Laboratory of Sichuan Province, College of Atmospheric Sciences, Chengdu University of Information Technology, Chengdu, China

Abstract Land surface albedo is a significant parameter for maintaining a balance in surface energy. It is also an important parameter of bare soil surface albedo for developing land surface process models that accurately reflect diurnal variation characteristics and the mechanism behind the solar spectral radiation albedo on bare soil surfaces and for understanding the relationships between climate factors and spectral radiation albedo. Using a data set of field observations, we conducted experiments to analyze the variation characteristics of land surface solar spectral radiation and the corresponding albedo over a typical Gobi bare soil underlying surface and to investigate the relationships between the land surface solar spectral radiation albedo, solar elevation angle, and soil moisture. Based on both solar elevation angle and soil moisture measurements simultaneously, we propose a new two-factor parameterization scheme for spectral radiation albedo over bare soil underlying surfaces. The results of numerical simulation experiments show that the new parameterization scheme can more accurately depict the diurnal variation characteristics of bare soil surface albedo than the previous schemes. Solar elevation angle is one of the most important factors for parameterizing bare soil surface albedo and must be considered in the parameterization scheme, especially in arid and semiarid areas with low soil moisture content. This study reveals the characteristics and mechanism of the diurnal variation of bare soil surface solar spectral radiation albedo and is helpful in developing land surface process models, weather models, and climate models.

1. Introduction

Almost one quarter of the Earth's total land surface consists of arid and semiarid areas distributed across every continent. These areas are nearly completely covered by a representative bare soil underlying surface. Moreover, climate change in these areas has become an important and essential factor in global change because of the sensitivity and fragility of these terrestrial ecosystems (Huang et al., 2012; Rotenberg & Dan, 2010). Land surface processes in arid and semiarid areas significantly influence local and regional weather and climate (Huang et al., 2012, 2013; Rotenberg & Dan, 2010; Xue & Shukla, 1993). However, a striking warming trend in arid and semiarid areas has become evident over the past century. This enhanced semiarid warming trend may cause these regions to become drier and warmer (Huang et al., 2012). Using historical data to bias-correct CMIP5 projections, dryland expansion will be augmented unless greenhouse gas concentrations are controlled (Huang et al., 2015). The increasing aridity, enhanced warming, and rapidly expanding human population will exacerbate the risk of land degradation and desertification in the near future in the drylands of developing countries (Huang et al., 2015, 2017).

Land surface albedo is an important parameter for land surface energy and water balance and for the formation and evolution of weather and climate (Charney, 1975; Charney et al., 1977; Trenberth & Fasullo, 2009; Trenberth et al., 2009; Wang et al., 2001, 2002a, 2002b; Zheng et al, 2012, 2014, 2015). Many previous studies have reported that the deviations in calculating land surface albedo can lead to land surface and air temperature biases, which then result in the changes to weather and climate forecasts (Charney, 1975; Charney et al., 1977; Lean & Rowntree, 1993; Trenberth & Fasullo, 2009). Albedo is an important parameter in land surface process models (LSMs; Bonan, 1996; Dai et al., 2003; Dickinson et al., 1993; Oleson et al., 2010, 2013; Sellers et al., 1986; Xue et al., 1991, 1996). Soil texture, soil color, and soil moisture are the key factors that affect bare soil surface albedo calculation in LSMs. So far, however, the parameterization schemes available for bare soil surface albedo are unsatisfactory. The schemes adopted in LSMs include the energy ratio values of spectral radiation that account for global radiation, the initial values of spectral radiation albedos, the failure to consider effect factors, and so on (Henderson-Sellers et al., 1993; Zheng et al., 2014, 2015).

Several studies have reported that the diurnal variation characteristics of bare soil surface albedo are closely related to solar elevation angle (Idso et al., 1975; Liu et al., 2008; Paltridge & Platt, 1981; Roxy et al., 2010; Tsvetsinskaya et al., 2002; Wang et al., 2004; Zhang & Huang, 2004a, 2004b; Zheng et al., 2014). Solar elevation angle has much more important effect on the diurnal variation characteristics of bare soil land surface albedo than the soil moisture in arid and semiarid areas with low soil moisture content (Bao et al., 2007; Idso et al., 1975; Zheng et al., 2014). However, the parameterization scheme of bare soil surface albedo considers only the influence of surface soil moisture. A single-factor scheme that considers only surface soil moisture cannot depict the diurnal variation characteristics of bare soil surface albedo, especially in arid and semiarid areas with low soil moisture content (Bao et al., 2007; Zheng et al., 2014). In this study, using a data set of field observations at a typical Gobi site, we analyzed the variation characteristics of land surface solar spectral radiation and the corresponding albedo and found out the relationships between land surface solar spectral radiation albedo, solar elevation angle, and surface soil moisture. Based on both solar elevation angle and soil moisture simultaneously, a two-factor set of parametric formulas for bare soil surface solar spectral radiation albedo were proposed. Numerical simulation experiments were performed to investigate the performance of the new parametric formulas.

The rest of this paper is organized as follows. Section 2 introduces the field observation experiment site, the data sources, the model, and the design of the numerical simulation experiments. Section 3 presents the results, including the analysis of the variation characteristics of bare soil surface solar spectral radiation and the corresponding albedo, the relationships between spectral radiation albedo, solar elevation angle, and surface soil moisture; and a comparative analysis of the numerical simulation results using the new parameterization schemes and the previous schemes. A discussion is provided in section 4, and section 5 concludes the paper.

2. Data and Methods

2.1. Field Observation Experiment and Data Sources

The Field Experiment on Air-Land Interaction in the Arid Area of Northwest China (NWC-ALIEX) has been ongoing continuously for the past 15 years (Huang et al., 2013; Zhang & Huang, 2004a; Zhang et al., 2002a, 2002b, 2005). NWC-ALIEX is used for scientific research into land-air interactions at typical underlying surfaces in the arid and semiarid areas in northwestern China. The Gobi landscape is a typical representative of the geomorphic features of large area in northwestern China, which covers a vast area. A field observation experiment was conducted at the Gobi site during the intensive observation period (IOP) from 20 September to 23 October 2010. The data set of from 22 September to 21 October 2010 was used for the analysis in this paper. The study area was located at 94°31′E, 40°10′N to the west of Dunhuang City, Gansu Province, Northwestern China at an altitude of 1,150 m, as shown in Figure 1. The Gobi site has a high frequency of clear sky conditions and a mixture of sand and gray-gravel plains form an open and unobstructed landscape. The environment surrounding the site is characterized by bare, flat, and homogeneous surface that represent the larger Gobi area. The upper surface of the Gobi site is predominantly composed of small stones, while fine sand composes the lower surface. The site's climate type is typical of a continental drought zone. Much more detailed information about the field observation site, its climate type, and its environment can be found in Wei et al. (2006), Huang et al. (2013), and Zheng et al. (2015, 2017).

Land surface downward and upward global radiation (GR) (280–2,800 nm) and spectral radiation (SR), including both ultraviolet radiation (UV) (285–395 nm) and visible radiation (VIS) (400–700 nm) were measured on a horizontal plane simultaneously with soil moisture at different depths (5, 10, 20, and 80 cm). The

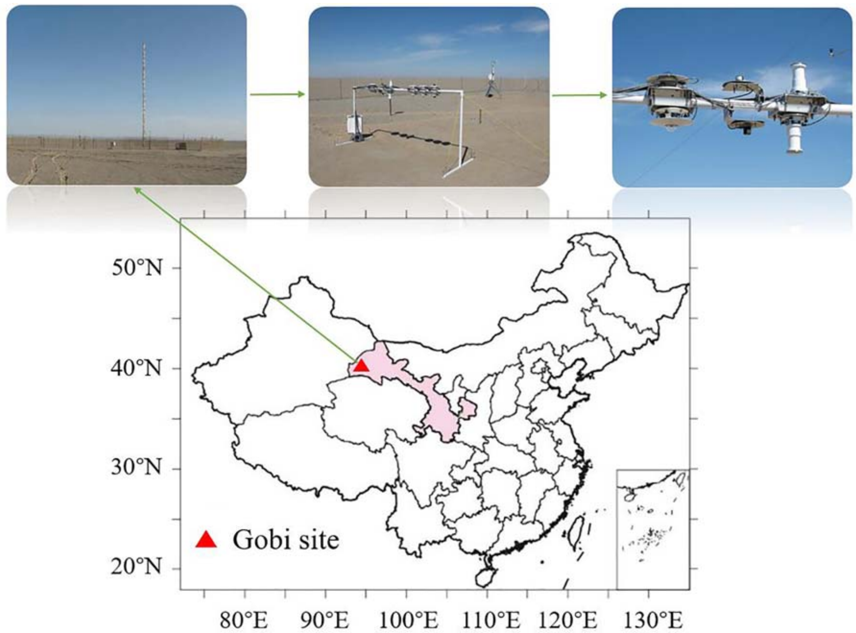

Figure 1. Spatial distribution of the field observation Gobi site.

GR and SR used to calculate the bare soil surface albedo were measured by high precision solar radiometers manufactured by Eppley Laboratory, Inc., Newport, RI, mounted on a 1.5 m high horizontal platform, as shown in Figure 1. The soil moisture was measured by a QP-SS (accuracy: $\pm$1% m^3/m^3, Elemental Scientific Inc., Omaha, NE). Measurements were taken every 1 min. The data were then averaged over 30 min to reduce noise. All the data were recorded using a DT600 data logger (DataTaker Inc., Scoresby, VIC, Australia) fitted with a Personal Computer Memory Card International Association memory card. Data were downloaded, inspected for quality, and processed into daily files. Over the course of the field observation experiment, the radiometer sensors were checked and cleaned every day to remove water droplets, dust, and other materials from the radiometer sensor domes. Detailed information about the specifications of the measurement instruments and the technical parameters of the land surface solar spectral radiation used at the Gobi site during the IOP can be found in supporting information Table S1.

First, data sets containing the land surface solar spectral radiation and the 5 cm depth surface soil moisture measurements from 22 September to 21 October 2010 were used to analyze the variations in land surface solar spectral radiation and the corresponding albedo as well as the relationships between the albedos of GR and SR and other factors. The other data sets (from 1 to 30 August 2009), including the land surface temperature, surface downward and upward shortwave and longwave radiation, and sensible heat flux, were used to verify the model simulation results. Note that near-infrared radiation (NIR) was not measured directly because the NIR radiometer was unavailable. Based on methods used in previous studies (Escobedo et al., 2011; Zheng et al., 2015), the missing NIR radiation irradiance can be indirectly estimated from the other waveband measurement irradiances. Hence, the NIR (700–2,800 nm) irradiance values used in this work were indirectly estimated using the equation NIR = GR – UV – VIS. Some tiny errors were ignored here.

Based on previous studies (Cañada et al., 2000; Fligge et al., 2001; Foyo-Moreno et al., 1998; Geiger et al., 2002; Iqbal, 1983; Koronakis et al., 2002; Ogunjobi & Kim, 2004; Shi et al., 2008; Wang et al., 2010; Zheng et al., 2015), quality control (QC) for the field observation experiments data sets was guaranteed. Much more detailed information concerning the methods for QC and the NWC-ALIEX data quality were described in previous studies (Wang et al., 2010; Zheng et al., 2015, 2017; Zhou & Huang, 2011). All the measurement instruments used in this study were calibrated by standard procedures both before and after the field observation experiments. Calibration of all measurement instruments was performed by a professional engineer from the China Meteorological Administration (CMA), which is the calibration agency in China officially authorized by the World Meteorological Organization (WMO) to ensure the precision of measurement instruments before conducting field observation experiments.

Table 1
Model Configuration Information

Grid ID	Center lon-lat	Domain dimension	Model resolution (km)	Time step (s)	Data resolution
1	94.52°E, 40.17°N	100 × 100	9	54	5 m
2	94.52°E, 40.17°N	88 × 88	3	54	2 m
3	94.52°E, 40.17°N	76 × 76	1	54	30 s

2.2. Model and Numerical Simulation Experiment Design

The Weather Research and Forecasting Model version 3.7.1 (WRFv3.7.1) with the Community Land Model version 4.0 (CLM4.0) as its land surface processes scheme was utilized to verify the simulation result. A three-nested grid system whose center was located at 94.52°E, 40.17°N was used in this study. In the vertical dimension, 35 unevenly spaced full eta levels were defined. Based on a series of tests, a set of physical options was selected within the WRF. The surface layer processes were resolved with the Revised MM5 surface layer scheme (Jiménez et al., 2012). The Community Land Model Version 4.0 (CLM4.0; Oleson et al., 2010) with 10 soil layers was used to resolve the land surface processes within the WRF. The planetary boundary layer processes were resolved with the Yonsei University scheme (YSU; Hong et al., 2006). The microphysics was calculated using the Lin scheme (Lin et al., 1983). The cumulus clouds were simulated with the Grell 3-D ensemble cumulus method (Grell et al., 2013). The Rapid Radiative Transfer Model (RRTMG; Iacono et al., 2008) was used to calculate longwave and shortwave radiation and their transfer within the atmosphere. The 6 h, 1° × 1° National Centers for Environmental Prediction Final Analysis (NCEP-FNL) from the Global Forecast System (GFS) was used to provide the initial and lateral boundary conditions for the WRF model. The model configuration, which includes center longitude-latitude, domain dimensions, spatial resolutions, and time steps, are listed in Table 1. In this paper, the selected simulation time for analysis extended from 0000 UTC 1 August 2009 to 1800 UTC 30 August 2009.

Three cases were designed that included different parameterization schemes of the bare soil land surface spectral radiation albedo. Case 1 considers only the soil moisture in the parameterization scheme of the bare soil surface albedo as prescribed for the CLM4.0 (Oleson et al., 2010). Case 2 is the new two-factor parameterization scheme based on both solar elevation angle and soil moisture simultaneously. Case 3 is a parameterization scheme that considers only the solar elevation angle. A comparative analysis of the GR albedo between the observed data and the simulated data of the Cases 1–3 is provided in section 3.

3. Results

3.1. Diurnal Variation Characteristics of Bare Soil Surface Spectral Radiation and the Corresponding Albedo

Based on the rule for separating different radiation wavebands in CLM4.0 (Oleson et al., 2010), the 700 nm wavelength is selected as the threshold to distinguish between visible radiation (less than 700 nm) and near-infrared radiation (greater than 700 nm). Hence, the observed UV (285–395 nm) and VIS (400–700 nm) were combined into a new VIS band (approximately 285–700 nm) as prescribed for CLM4.0. The NIR wavelength ranges from 700 to 2,800 nm.

Figure 2 shows the temporal evolution of the observed diurnal variation and daily-averaged VIS, NIR, and GR albedos at the Gobi field observation site during the IOP. As shown in Figure 2a, the diurnal variation characteristics of the VIS, NIR, and GR albedos are pronounced, showing approximately a U-shape. The VIS, NIR, and GR albedos are asymmetric matching the results of Song (1998), Wen et al. (2009), and Zheng et al. (2012, 2015). Morning albedos are larger than those in the afternoon (Figure 2a). The daily-averaged albedos were calculated according to a weight factor (the surface reflected radiation flux); therefore, the weighted averaged surface albedos were calculated according to the equation used in Zhang and Huang (2004b). The daily-averaged VIS, NIR, and GR albedos are essentially constant (Figure 2b), with values of 0.22, 0.26, and 0.24, respectively. More detailed statistical characteristics of the daily-averaged VIS, NIR, and GR albedos at the Gobi field observation site during the IOP can be found in Table 2. Note that the observed values of the Gobi bare soil surface albedo for the NIR are not twice those of the VIS over bare soil underlying surfaces as prescribed in most LSMs (Bonan, 1996; Dai et al., 2003; Dickinson et al., 1993; Oleson et al., 2010, 2013; Sellers et al., 1986; Xue et al., 1991, 1996). These results match the results from our previous studies (Zheng et al., 2012, 2015).

Figure 3 shows the temporal evolution of the diurnal variation and daily-averaged energy ratios of VIS and NIR account for GR at the Gobi field observation site during the IOP. The diurnal variations of energy ratios

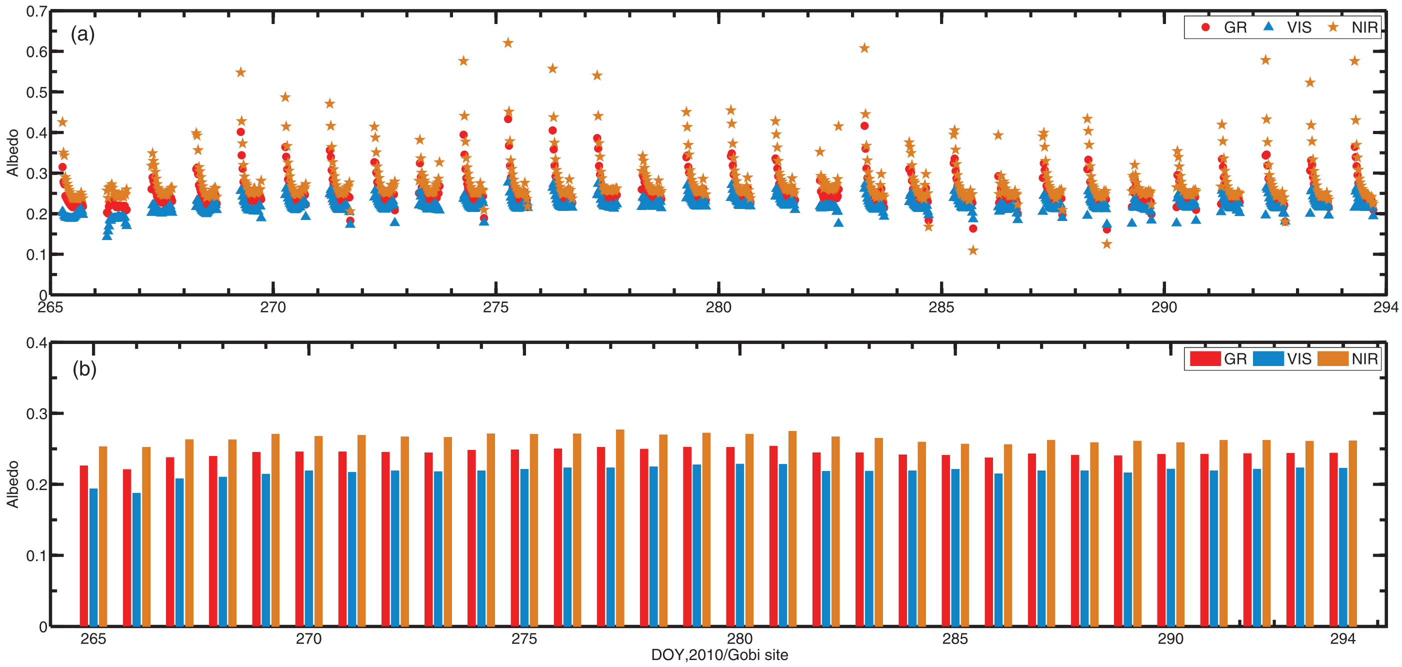

Figure 2. Temporal evolution of the observed albedos of GR, VIS, and NIR at the Gobi field observation site during the IOP, (a) each measured albedo and (b) the daily-averaged albedo, respectively.

of VIS/GR and NIR/GR are pronounced, as shown in Figure 3a. The diurnal variation curve of the NIR/GR energy ratio has a single apex: high at midday and low in the morning and evening. In contrast to the diurnal variation characteristics of energy ratio of the NIR/GR, the diurnal variation of the VIS/GR energy ratio shows opposite variation characteristics; it is high in the morning and evening and low at midday. This result occurs because different atmospheric compositions absorb different wavelengths of solar radiation. The daily-averaged VIS/GR and NIR/GR energy ratio are almost constant at the Gobi site (Figure 3b), with values of approximately 46.3% and 54.7%, respectively. Figure 3b shows that the VIS/GR and NIR/GR energy ratios do not account for 50% of the total as prescribed by some LSMs (Bonan, 1996; Dai et al., 2003; Dickinson et al., 1993; Oleson et al., 2010, 2013; Sellers et al., 1986; Xue et al., 1991, 1996). Instead, the VIS/GR energy ratio is less than 50%, but the NIR/GR ratio is greater than 50%. More detailed statistics of the characteristics of the daily-averaged VIS/GR and NIR/GR energy ratios at the Gobi site are summarized in Table 3.

3.2. Relationships Between Bare Soil Surface Albedo, Solar Elevation Angle, and Land Surface Soil Moisture

As described in the study of Zheng et al. (2015), bare soil surface albedo is a function of specific soil color classes and land surface soil moisture but independent of solar elevation angle in many LSMs (Bonan, 1996; Dai et al., 2003; Dickinson et al., 1993; Oleson et al., 2010, 2013; Sellers et al., 1986; Xue et al., 1991, 1996). Soil moisture has been accepted as one of the most important external effect factors for the variation characteristics of bare soil surface albedo. The relationship between bare soil surface albedo and soil moisture

Table 2
Statistical Characteristics of the Daily-Averaged VIS, NIR, and GR Albedo Values at the Gobi Field Observation Site During the IOP

	Statistical characteristics of the values of daily-averaged albedo				
	Min. value	Max. value	Avg. value	Var. value	Std. dev. value
VIS	0.187	0.228	0.217	0.00007	0.0087
NIR	0.251	0.276	0.264	0.00003	0.0063
GR	0.221	0.253	0.243	0.00004	0.0069

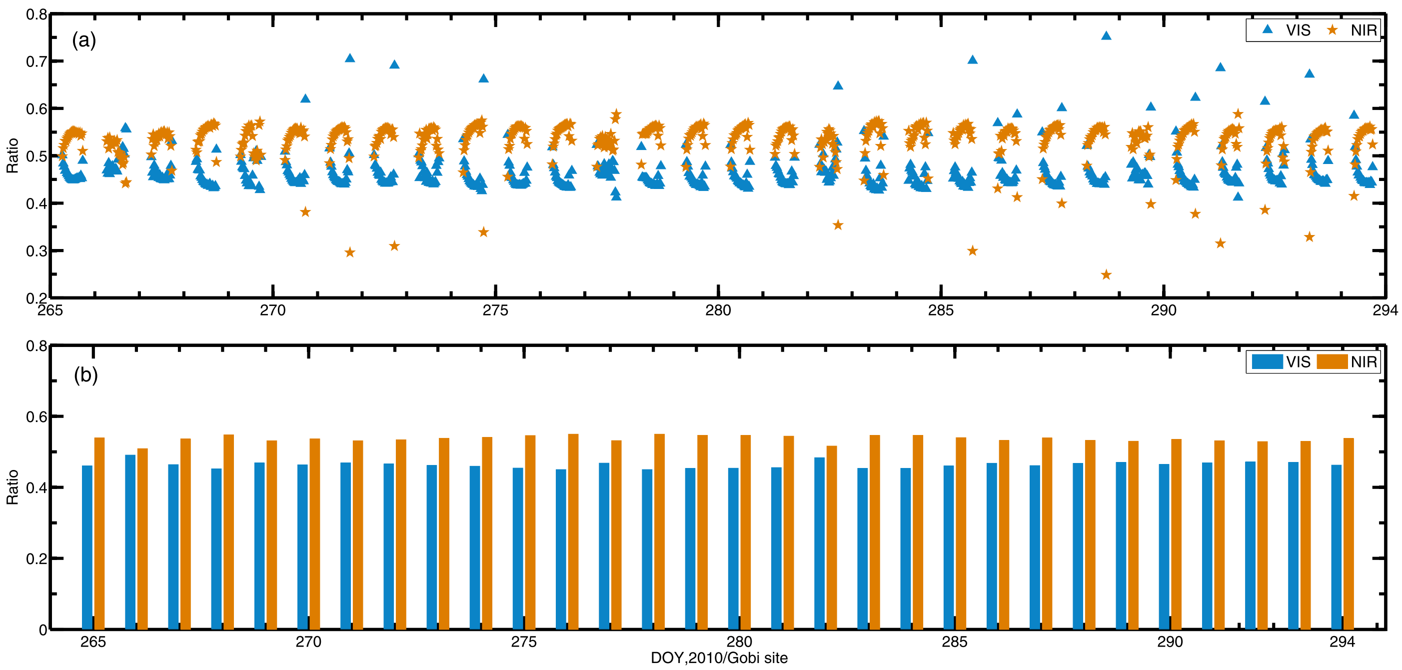

Figure 3. Temporal evolution of the energy ratios of VIS and NIR account for GR at the Gobi field observation site during the IOP, (a) each measured energy ratio and (b) the daily-averaged energy ratio, respectively.

has attracted the attention of many researchers (Guan et al., 2009; Liu et al., 2008; Roxy et al., 2010; Zhang et al., 2003; Zhang & Huang, 2004b; Zheng et al., 2014). Moreover, many previous studies have discussed the relationship between bare soil surface albedo and solar elevation angle and revealed that the solar elevation angle also has a significant effect on bare soil surface albedo variation characteristics and trends, especially on diurnal variation characteristics (Idso et al., 1975; Liu et al., 2008; Roxy et al., 2010; Zhang et al., 2003; Zhang & Huang, 2004b; Zheng et al., 2014). However, thus far, solar elevation angle has not been considered in some land surface process model (CLM/CoLM) in the albedo parameterization scheme for bare soil land surfaces. As shown in Figure 2a, the diurnal variation characteristics of SR and GR surface albedos have a pronounced approximately U-type-shaped curve at the Gobi site. At 5 cm depth, the surface soil moisture is very low at the Gobi site because of its drought climate. The surface water content was nearly zero during the IOP, as shown in supporting information Figure S1. According to the parameterization formula of bare soil surface albedo in the CLM4.0 (Oleson et al., 2010), there is no obvious U-shape of the diurnal variation of albedo (Figure 2a); instead, the graph shows a line with a constant slope because the soil moisture at surface is always low. Hence, the parameterized formula cannot exactly depict the diurnal variation characteristics of the bare soil surface albedo at a given moment. In other words, a parameterization scheme that considers only surface soil moisture will not reflect the essential physical mechanism of the diurnal variations of surface albedo at bare soil underlying surfaces. Apparently, for one kind of bare soil underlying surface in an area over a brief period, soil moisture is not the only significant effect factor controlling the diurnal variation characteristics and trends of bare soil surface albedo. Solar elevation angle may be another important effect factor controlling the diurnal variation characteristics and trends of bare soil

Table 3
Statistical Characteristics of the Daily-Averaged VIS/GR and NIR/GR Energy Ratio Values at the Gobi Field Observation Site During the IOP

	Statistical characteristics of the values of energy ratio				
	Min. value	Max. value	Avg. value	Var. value	Std. dev. value
VIS/GR	0.450	0.491	0.463	0.00008	0.0093
NIR/GR	0.509	0.550	0.547	0.00008	0.0093

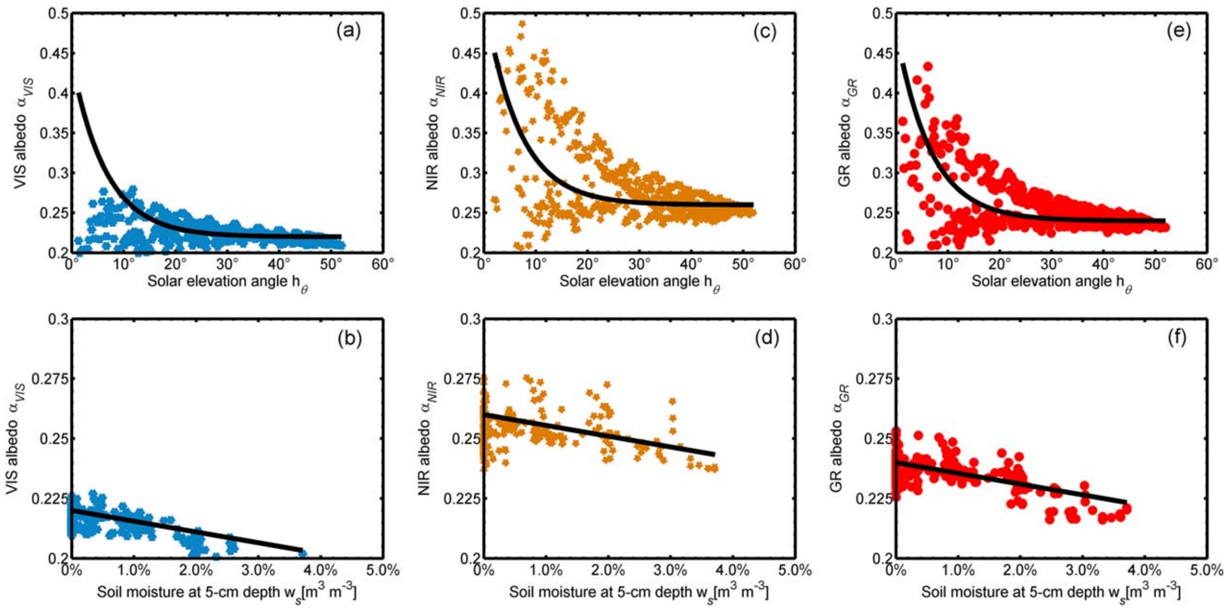

Figure 4. Relationships between the ground surface VIS, NIR, and GR albedos and the solar elevation angle, and between the albedos and the surface soil moisture at 5 cm depth at the Gobi field observation site during the IOP, (a) and (b) the VIS, (c) and (d) the NIR, and (e) and (f) the GR, respectively. The solar elevation angle is shown in degree units, and the soil moisture at a 5 cm depth is shown in m^3/m^3 units.

surface albedo, especially in arid and semiarid areas with low soil moisture content. To precisely depict the diurnal variation characteristics of bare soil surface albedo, a new two-factor parameterization scheme based on both solar elevation angle and surface soil moisture simultaneously is necessary.

We hypothesize that the solar elevation angle and soil moisture are independent of each other. When we investigate the impact of solar elevation angle on albedo, the influence of soil moisture must be removed, and vice versa. According to previous studies (Zhang et al., 2003; Zheng et al., 2014), the data that surface soil moisture values were below 1.5% m^3/m^3 (which is regarded as a dry bare soil condition) were selected to analyze the influence of solar elevation angle on bare soil surface albedo. By the same token, the data that the solar elevation angle was greater than 40° were selected to discuss the variation characteristics and trends of bare soil surface albedo affected only by the soil moisture. Figure 4 shows the relationships between the VIS, NIR, and GR bare soil surface albedos and the solar elevation angle, and the relationships between the albedos and the surface soil moisture at 5 cm depth. As shown in Figures 4a, 4c, and 4e, the VIS, NIR, and GR bare soil surface albedos decrease as the solar elevation angle increases and tend to remain constant when the solar elevation angle is greater than 40°. There are exponential relationships between the bare soil surface albedos and the solar elevation angle, which accords with the results of Idso et al. (1975), Zhang et al. (2003), Liu et al. (2008), and Zheng et al. (2014). Surface albedos decrease as the surface soil moisture at a 5 cm depth increases, and they show a linear dependence on soil moisture (Figures 4b, 4d, and 4f), which also accords with the results of some previous studies (Zhang et al., 2003; Zheng et al., 2014). Based on Figure 4, the VIS, NIR, and GR fitted formulas are achieved using the least squares method, as listed below.

The relationships between the bare soil surface albedos and the solar elevation angle are

$$\alpha_{VIS-1}=0.22+0.22\times\exp\left(-0.15\times h_\theta\right), \tag{1}$$

$$\alpha_{NIR-1}=0.26+0.26\times\exp\left(-0.15\times h_\theta\right), \tag{2}$$

$$\alpha_{GR-1}=0.24+0.24\times\exp\left(-0.15\times h_\theta\right), \tag{3}$$

where α_{VIS-1}, α_{NIR-1}, and α_{GR-1} are the VIS, NIR, and GR bare soil surface albedos, respectively, when only the solar elevation angle is considered, and h_θ is the solar elevation angle in degree units. The correlation coefficients of equations (1)–(3) are 0.449, 0.503, and 0.609, and the root mean square errors are 0.012, 0.039, and 0.026, respectively.

Similarly, the relationships between the bare soil surface albedos and the surface soil moisture at 5 cm depth are

$$\alpha_{VIS-2}=0.22-0.45\times ws, \quad (4)$$

$$\alpha_{NIR-2}=0.26-0.45\times ws, \quad (5)$$

$$\alpha_{GR-2}=0.24-0.45\times ws, \quad (6)$$

where α_{VIS-2}, α_{NIR-2}, and α_{GR-2} are the VIS, NIR, and GR bare soil surface albedos, respectively, when only the surface soil moisture is considered only, and *ws* is the surface soil moisture at a 5 cm depth in m^3/m^3 units. The correlation coefficients of equations (4)–(6) are 0.622, 0.621, and 0.619, and the root mean square errors are 0.0037, 0.0080, and 0.0056, respectively. The fitted formulas (1)-(6) are only single-factor parameterization formulas; in the real word, however, both solar elevation angle and soil moisture influence on the bare soil surface albedo at the same time. Land surface soil moisture is almost always equal to zero ($ws=0$) in bare soil underlying surfaces in arid and semiarid areas. When $ws=0$ in the fitted formulas (4)-(6), these fitted formulas are equal to a constant ($\alpha_{VIS-2}=0.22$, $\alpha_{NIR-2}=0.26$, $\alpha_{GR-2}=0.24$). Hence, using these formulas, the bare soil surface albedo will be a constant in dry soil conditions and will not exhibit the U-shaped diurnal variation characteristics and trends as shown in Figure 2a. Obviously, this result is irrational. Instead, when the soil moisture is equal to zero ($ws=0$), the diurnal variation characteristics of bare soil surface albedo are controlled only by the solar elevation angle, as shown in the fitted formulas (1)-(3). Then, the diurnal variation characteristics of bare soil surface albedo show a U-shape as shown in Figure 2a. Therefore, we used the fitted formulas (1)-(3) to replace the constant result from the fitted formulas (4)-(6) as Zhang et al. (2003) and Zheng et al. (2014) done. Finally, the new two-factor parameterization scheme for bare soil surface albedos based on both solar elevation angle and soil moisture simultaneously are obtained as follows:

$$\alpha_{VIS}=0.22+0.22\times\exp\left(-0.15\times h_\theta\right)-0.45\times ws, \quad (7)$$

$$\alpha_{NIR}=0.26+0.26\times\exp\left(-0.15\times h_\theta\right)-0.45\times ws, \quad (8)$$

$$\alpha_{GR}=0.24+0.24\times\exp\left(-0.15\times h_\theta\right)-0.45\times ws, \quad (9)$$

where α_{VIS}, α_{NIR}, and α_{GR} are the VIS, NIR, and GR bare soil surface albedos, respectively, when the solar elevation angle and surface soil moisture are considered simultaneously. The fitted formulas (7)-(9) are the two-factor parametric equations required for accurate calculation.

3.3. Numerical Simulation Verification

In section 3.2, the two-factor parametric equations were proposed based on both solar elevation angle and soil moisture measurement simultaneously. A verification simulation was performed to evaluate the performance of the new two-factor parameterization scheme. The design of the model and the numerical simulation experiments design were introduced in section 2.2.

Figure 5 shows a comparative analysis of the diurnal variation of the albedos of GR between the observed measurements and those simulated by Cases 1–3. As shown in Figure 5a, the value of the bare soil surface albedo of GR simulated by the original parameterization scheme prescribed in the CLM4.0 (Case 1) is greater than the observed value. Moreover, the diurnal variation trend of GR albedo is approximately a straight line rather than a U-shape. When the solar elevation angle and surface soil moisture are considered in the parameterization scheme simultaneously (Case 2), the U-shape of the diurnal variation characteristics of the bare soil surface albedo of GR can be reproduced successfully, but the value of the GR albedo is less than the observed value (Figure 5a). The low GR albedo simulated by Case 2 is shown because the simulated surface soil moisture at 5 cm depth is greater than the observed soil moisture, as shown in Figure 6. Higher surface soil moisture leads to lower bare soil surface albedo, but the U-shape diurnal variation characteristics and trends are consistent with the observations. Because the observed surface soil moisture at the 5 cm depth is zero (Figure 6), soil moisture has no impact on the bare soil surface albedo. If we consider only the impact of the solar elevation angle in the parameterization scheme as in Case 3, both the GR value and the diurnal variation characteristics of the bare soil surface albedo are very similar to the observed measurements, as shown in Figure 5b.

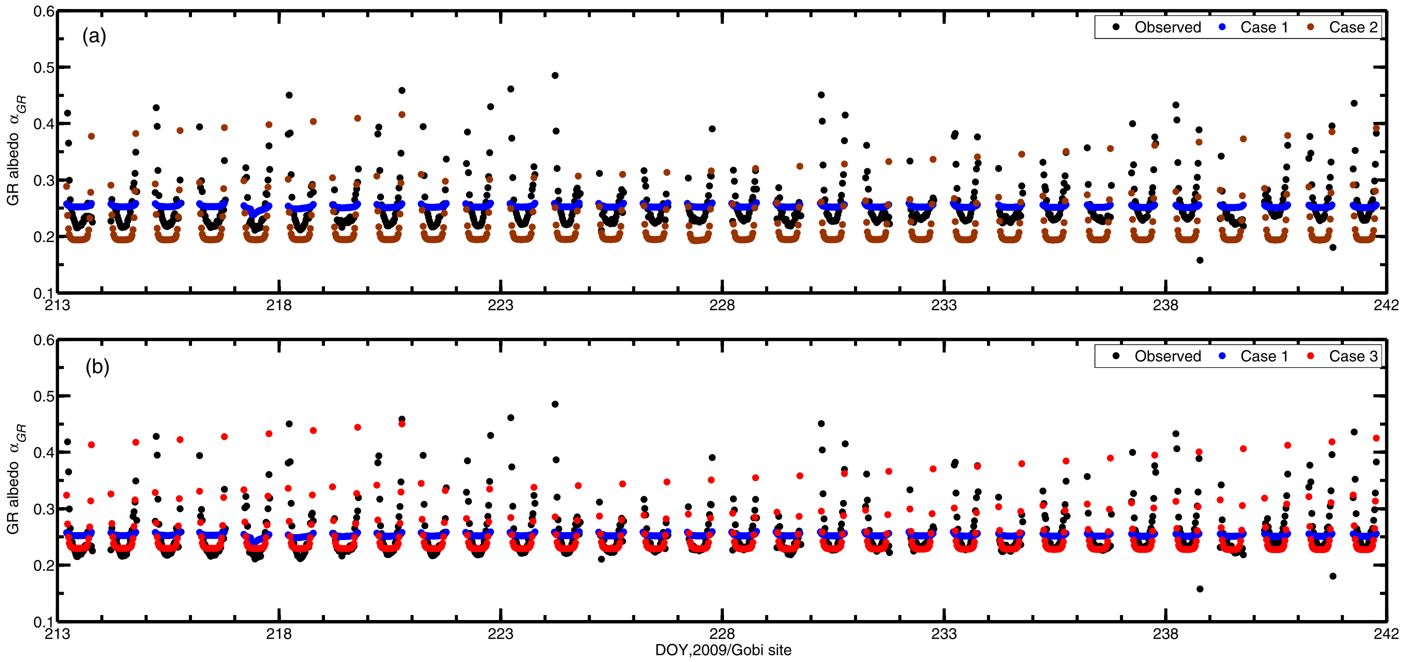

Figure 5. Comparative analysis of the diurnal variation of GR albedos between the observed measurements and those simulated by Cases 1–3.

Figure 7 shows a comparative analysis of the temporal evolution of USR between the observed measurements and those simulated by Cases 1–3. As shown in Figure 7, the simulated values and the variation characteristics and trends of USR are much better simulated in Case 3 than in the other cases. Figure 8 shows a comparative analysis of the differences in the daily-averaged upward shortwave radiation (USR) and sensible heat flux (Hs) between the observed values and those simulated by Cases 1–3. The results indicate that the simulated values of the parameterization scheme based on solar elevation angle and soil moisture simultaneously (Case 2) are closer to the observed values than the values using the parameterization scheme that consider only soil moisture (Case 1). However, when the simulated soil moisture value is equal to the observed value, the USR values simulated by Case 3 will be much closer to the observed value than

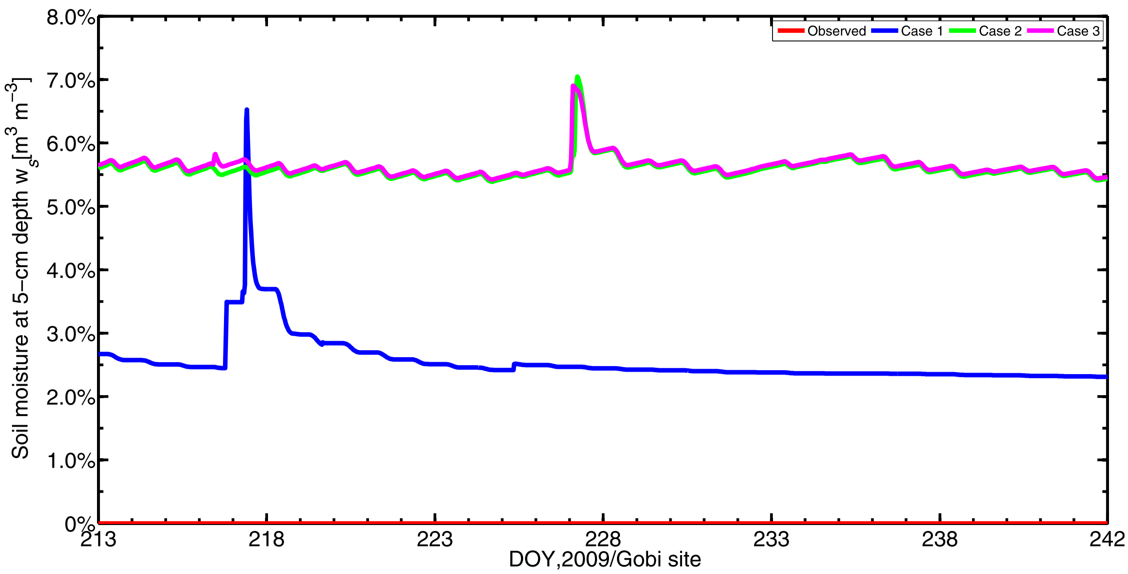

Figure 6. Comparative analysis of the temporal evolution of surface soil moisture at 5 cm depth between the observed measurements and those simulated by Cases 1–3. The soil moisture at a 5 cm depth is shown in m^3/m^3 units.

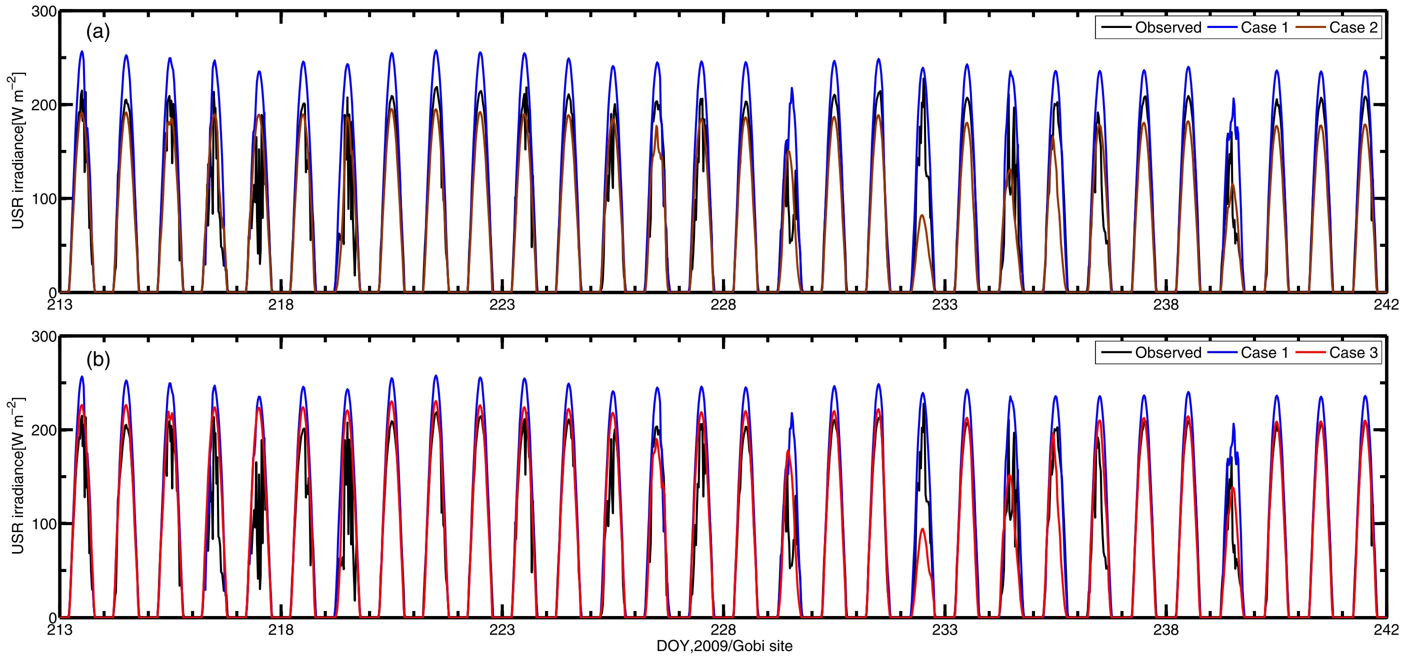

Figure 7. Comparative analysis of the temporal evolution of USR between the observed measurements and those simulated by Cases 1–3. The USR and Hs measurements are shown in W/m^2 units.

those simulated by Cases 1 and 2, as shown in Figure 8. The parameterization schemes that consider solar elevation angle can obtain better simulation results than the scheme that considers only the soil moisture for bare soil surface albedo. A comparative analysis of the temporal evolution of USR and Hs between the observed measurements and those simulated by Cases 1–3 shows similar conclusions to those depicted in Figure 8, as shown in supporting information Figure S2.

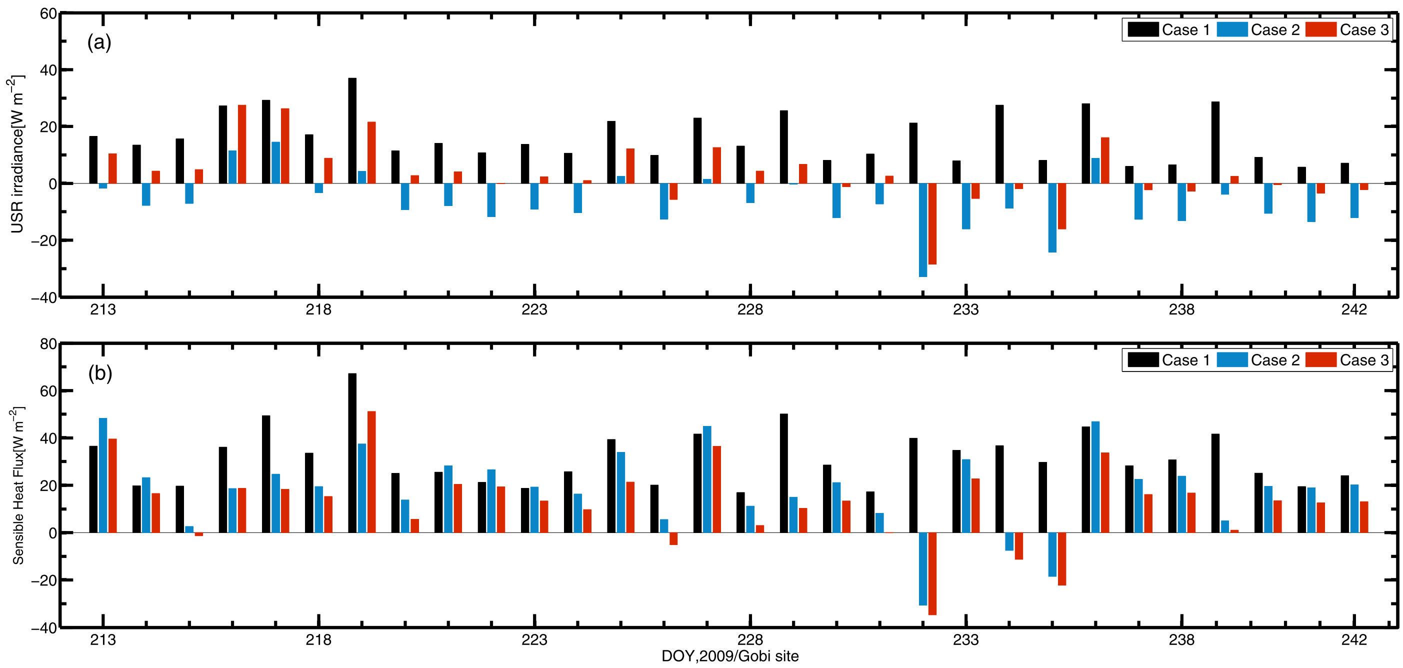

Figure 8. Comparative analysis of the differences of daily-averaged USR and Hs between the observed measurements and those simulated by Cases 1–3, (a) the USR irradiance, and (b) the sensible heat flux. The USR and Hs are shown in W/m^2 units.

In conclusion, the new two-factor parameterization scheme based on both solar elevation angle and soil moisture simultaneously can better reproduce the diurnal variation characteristics of the bare soil surface albedo than the previous single-factor scheme based only on soil moisture as prescribed for the CLM4.0, especially in arid and semiarid areas with low soil moisture content. Solar elevation angle is an important factor for bare soil surface albedo parameterization, and it must be considered in parameterization schemes in land surface process models, weather models, and climate models.

4. Discussion

In section 3, based on the data sets of field observation experiment during the IOP at the Gobi site in northwestern China, we discussed the diurnal and daily-averaged variation characteristics and trends of bare soil surface solar spectral radiation and the corresponding albedo and provided a two-factor parameterization scheme for calculating bare soil surface spectral albedo. The new two-factor parameterization scheme was implemented in the land surface process model (CLM4.0). Subsequently, model simulation results indicated that the solar elevation angle is a significant factor for determining the diurnal variation characteristics of bare soil surface albedo. This result is very important. However, the timescale of the data sets used in this study was relatively short. Consequently, our results may have some uncertainties. Moreover, the Gobi landform is only one type of bare soil underlying surfaces in arid and semiarid areas in northwestern China. Desert and bare loess are also representative bare soil underlying surfaces, as mentioned in our previous work in Zheng et al. (2015). Therefore, another longer-timescale field observation experiments should be conducted to consider different kinds of bare soil underlying surfaces in arid and semiarid areas in the future. Such studies would be helpful to enrich and improve the parameters and parameterization schemes of bare soil surface albedo in land surface process models.

The WRF with CLM4.0 as its land surface processes scheme was utilized to conduct the simulation verification in this study. Here, we analyzed only the USR and Hs differences between the new parameterization schemes and the original scheme. In the future work, we are going to plan to investigate additional influences from atmospheric circulation, precipitation, air humidity, land and air temperature, land surface energy, and water balance, and to discuss local and regional weather and climate. The new two-factor parameterization scheme also will be ported into offline land surface process models, such as CLM or CoLM to check the simulation results using the single point site. In conclusion, much more effort is required to improve land surface process models in the future.

5. Conclusions

In this study, using the data sets acquired through field observation from the NWC-ALIEX in northwestern China, we analyzed the diurnal and daily-averaged variation characteristics of bare soil surface solar spectral radiation and the corresponding albedo and proposed a new two-factor parameterization scheme for calculating bare soil surface albedo based on both solar elevation angle and soil moisture simultaneously. The main results are summarized as follows.

The global and spectral radiation albedos have obvious daily and diurnal variation characteristics. The diurnal variation characteristics of the VIS, NIR, and GR albedos show an approximate U-shape. The VIS, NIR, and GR albedos are asymmetric, and the values of the VIS, NIR, and GR daily-averaged albedos are 0.22, 0.26, and 0.24, respectively, and the daily-averaged albedos remain almost constant. The actual observed value of the bare soil surface albedo for the NIR is not twice that of the VIS as prescribed for bare soil underlying surfaces in some LSMs; instead, the daily-averaged energy ratios of VIS/GR and NIR/GR are almost constant at the Gobi site. The values of the daily-averaged energy ratios of VIS/GR and NIR/GR were approximately 46.3% and 54.7%, respectively. This result means that the energy ratios of VIS/GR and NIR/GR do not account for 50% of the total as prescribed in some LSMs. These results constitute two large discrepancies between the observed values and that the values prescribed in LSMs that should be given more attention in the future.

Using the field observation experiment data sets, we analyzed the relationships between the bare soil surface albedos of GR and SR and the solar elevation angle as well as the relationships between the albedos and soil moisture. We proposed a new two-factor parameterization scheme for calculating bare soil surface albedo based on both solar elevation angle and soil moisture simultaneously. The results of numerical simulation experiments verified that the new two-factor parameterization scheme can reproduce the true values and diurnal variation characteristics of the bare soil surface albedo. The upward shortwave radiation and sensible heat flux values simulated by the two-factor parameterization scheme are also greatly improved over those that simulated by the single-factor scheme that considers only the influence of soil moisture.

Our results imply that the solar elevation angle is also a significant factor that should be included in bare soil surface albedo parameterization scheme over typical bare soil underlying surfaces, especially in arid and semiarid areas with low soil moisture content. Clarifying the importance of solar elevation angle not only provides a useful approach to understanding bare soil surface albedo but also a possible way to reduce biases in simulations of bare soil surface albedo, land surface energy, and water balance. This work reveals the characteristics, rules, and mechanism of diurnal variation of bare soil surface solar spectral radiation and the corresponding albedo, and it will be helpful for developing land surface process models, and may even benefit weather and climate models.

Acknowledgments
The field observation experiment data set used in this study, which is supported by the National Natural Science Foundation of China and Ministry of Science and Technology of the People's Republic of China, can be accessed from Data Archive & Sharing Network for Resource and Environment Projects of 973 Program (http://www.973geodata.cn/dataservice/index.jsp?url=/dataservice/index.jsp&pid=2009CB421400&pn=1). The data used to provide the initial and lateral boundary conditions (6 h, 1° × 1°) for the WRF model are available through the database of National Centers for Environmental Prediction Final Analysis (NCEP-FNL) from the Global Forecast System (GFS) (https://rda.ucar.edu/datasets/ds083.2/). We are very grateful to the editor and anonymous reviewers for their careful reviews and valuable comments, which led to substantial improvement of this work. This study is jointly supported by the National Key R&D Program of China grant (2016YFA0602701), the Opening Fund of Key Laboratory for Land Surface Process and Climate Change in Cold and Arid Regions grant (LPCC2016001), the project supported by State Key Laboratory of Earth Surface Processes and Resource Ecology grant (2017-KF-14), and the National Natural Science Foundation of China grants (41375001, 41405063, and 41275011).

References

Bao, Y., Lv, S. H., Ao, Y. H., Li, Y. H., Meng, X. H., Yang, S. P., & Chen, X. L. (2007). Improvement of surface albedo parameterization over bare soil on surface radiation and thermal process modeling [in Chinese with English abstract]. *Acta Energiae Solaris Sinica*, *28*(7), 775–782.

Bonan, G. B. (1996). *A land surface model (LSM version 1.0) for ecological, hydrological, and atmospheric studies: Technical description and user's guide* (NCAR Tech. Note NCAR/TN-417+STR, pp. 29–30). Boulder, CO: National Center for Atmospheric Research.

Cañada, J., Pedrós, G., López, A., & Boscá, J. V. (2000). Influences of the clearness index for the whole spectrum and of the relative optical air mass on UV solar irradiance for two locations in the Mediterranean area, Valencia and Cordoba. *Journal of Geophysical Research*, *105*, 4759–4766. https://doi.org/10.1029/1999JD901106

Charney, J., Quirk, W. J., Chow, S. H., & Kornfield, J. (1977). A comparative study of the effects of albedo change on drought in semi-arid regions. *Journal of Atmosphere Sciences*, *34*, 1366–1385. https://doi.org/10.1175/1520-0469(1977)034<1366:ACSOTE>2.0.CO;2

Charney, J. G. (1975). Dynamics of deserts and drought in the Sahel. *Quarterly Journal of the Royal Meteorological Society*, *101*(428), 193–202. https://doi.org/10.1002/qj.49710142802

Dai, Y. J., Zeng, X. B., Dickinson, R. E., Baker, I., Bonan, G. B., Bosilovich, M. G., . . . Yang, Z. L. (2003). The common land model. *Bulletin of the American Meteorological Society*, *84*(8), 1013–1023. https://doi.org/10.1175/BAMS-84-8-1013

Dickinson, R. E., Henderson-Sellers, A., & Kennedy, P. J. (1993). *Biosphere-atmosphere transfer scheme (BATS) version 1e as coupled to the NACR community model* (NCAR Tech. Note NCAR/TN-387+STR, pp. 22–27). Boulder, CO: National Center for Atmospheric Research.

Escobedo, J. F., Eduardo, N. G., Amauri, P. O., & Jacyra, S. (2011). Ratios of UV, PAR and NIR components to global solar radiation measured at Botucatu site in Brazil. *Renewable Energy*, *36*, 169–178. https://doi.org/10.1016/j.renene.2010.06.018

Fligge, M., Solanki, S. K., Pap, J. M., Frohlich, C., & Wehrli, C. (2001). Variations of solar spectral irradiance from near UV to the infrared–measurements and results. *Journal of Atmospheric and Solar-Terrestrial Physics*, *63*(14), 1479–1487.

Foyo-Moreno, I., Vida, J., & Alados-Arboledas, L. (1998). Ground based ultraviolet (290–385 nm) and broadband solar radiation measurements in south eastern Spain. *International Journal of Climatology*, *18*, 1389–1400.

Geiger, M., Diabaté, L., Ménard, L., & Wald, L. (2002). A web service for controlling the quality of measurements of global solar radiation. *Solar Energy*, *73*(6), 475–480. https://doi.org/10.1016/S0038-092X(02)00121-4

Grell, T. A. J., Alabanza, A. M., Gaskell, K., & Aslan, K. (2013). Microwave-accelerated surface modification of plasmonic gold thin films with self-assembled mono layers of alkanethiols. *Langmuir*, *29*(43), 13209–13216. https://doi.org/10.1021/la402455x

Guan, X. D., Huang, J. P., Guo, N., Bi, J. R., & Wang, G. Y. (2009). Variability of soil moisture and its relationship with surface albedo and soil thermal parameters over the Loess Plateau. *Advances in Atmospheric Sciences*, *26*(4), 692–700. https://doi.org/10.1007/s00376-009-8198-0

Henderson-Sellers, A., Yang, Z. L., & Dickinson, R. E. (1993). The project for intercomparison of land-surface parameterization schemes. *Bulletin of the American Meteorological Society*, *74*(7), 1335–1349.

Hong, S. Y., Noh, Y., & Dudhia, J. (2006). A new vertical diffusion package with an explicit treatment of entrainment processes. *Monthly Weather Review*, *134*(9), 2318–2341.

Huang, J. P., Guan, X. D., & Ji, F. (2012). Enhanced cold-season warming in semi-arid regions. *Atmospheric Chemistry and Physics*, *12*, 5391–5398. https://doi.org/10.5194/acp-12-5391-2012

Huang, J. P., Ji, M. X., Liu, Y. Z., Zhang, L., & Gong, D. Y. (2013). An overview of arid and semi-arid climate change [in Chinese with English abstract]. *Advances in Climate Change Research*, *9*(1), 9–14. https://doi.org/10.3969/j.issn.1673-1719.2013.01.002

Huang, J. P., Yu, H. P., Dai, A. G., Wei, Y., & Kang, L. T. (2017). Drylands face potential threat under 2°C global warming target. *Nature Climate Change*, *7*, 417–422. https://doi.org/10.1038/nclimate3275

Huang, J. P., Yu, H. P., Guan, X. D., Wang, G. Y., & Guo, R. X. (2015). Accelerated dryland expansion under climate change. *Nature Climate Change*, *6*, 166–171. https://doi.org/10.1038/nclimate2837

Iacono, M. J., Delamere, J. S., Mlawer, E. J., Shephard, M. W., Clough, S. A., & Collins, W. D. (2008). Radiative forcing by long-lived greenhouse gases: Calculations with the AER radiative transfer models. *Journal of Geophysical Research*, *113*, D13103. https://doi.org/10.1029/2008JD009944

Idso, S. B., Jackson, R. D., Reginato, R. J., Kimball, B. A., & Nakayama, F. S. (1975). The dependence of bare soil albedo on soil water content. *Journal of Applied Meteorology*, *14*(1), 109–113.

Iqbal, M. (1983). *An introduction to solar radiation* (Vol. XVII, 390 pp.). New York, NY: Academic Press Inc.

Jiménez, P. A., Dudhia, J., González-Rouco, J. F., Navarro, J., Montávez, J. P., & García-Bustamante, E. (2012). A revised scheme for the WRF surface layer formulation. *Monthly Weather Review*, *140*(3), 898–918. https://doi.org/10.1175/MWR-D-11-00056.1

Koronakis, P. S., Sfantos, G. K., Paliatsos, A. G., Kaldellis, J. K., Garofalakis, J. E., & Koronaki, I. P. (2002). Interrelations of UV-global/global/diffuse solar irradiance components and UV-global attenuation on air pollution episode day in Athens, Greece. *Atmospheric Environment*, *36*(19), 3173–3181. https://doi.org/10.1016/S1352-2310(02)00233-9

Lean, J., & Rowntree, P. R. (1993). A GCM simulation of the impact of Amazonian deforestation on climate using an improved canopy representation. *Quarterly Journal of the Royal Meteorological Society*, *119*(511), 509–530. https://doi.org/10.1002/qj.49711951109

Lin, Y. L., Farley, R. D., & Orville, H. D. (1983). Bulk parameterization of the snow field in a cloud model. *Journal of Climate and Applied Meteorology*, *22*, 1065–1092.

Liu, H. Z., Wang, B. M., & Fu, C. B. (2008). Relationships between surface albedo, soil thermal parameters and soil moisture in the semi-arid area of Tongyu, Northeastern China. *Advances in Atmospheric Sciences*, *25*(5), 757–764. https://doi.org/10.1007/s00376-008-0757-2

Ogunjobi, K. O., & Kim, Y. J. (2004). Ultraviolet (0.280–0.400 μm) and broadband solar hourly radiation at Kwangju, South Korea: Analysis of their correlation with aerosol optical depth and clearness index. *Atmospheric Research*, *71*(3), 193–214. https://doi.org/10.1016/j.atmosres.2004.05.001

Oleson, K. W., Lawrence, D. M., Bonan, G. B., Drewniak, B., Huang, M. Y., Koven, C. D., . . . Yang, Z.-L. (2013). *Technical description of version 4.5 of the community land model (CLM)* (NCAR Tech. Note NCAR/TN-487+STR). Boulder, CO: National Center for Atmospheric Research.

Oleson, K. W., Lawrence, D. M., Bonan, G. B., Flanner, M., Kluzek, G. E., Lawrence, P., . . . Zeng, X. B. (2010). *Technical description of version 4.0 of the community land model (CLM)* (NCAR Tech. Note NCAR/TN-503+STR). Boulder, CO: National Center for Atmospheric Research.

Paltridge, G. W., & Platt, C. M. R. (1981). *The radiation processes in meteorology and climatology* (pp. 84–97). Beijing, China: Science Press.

Rotenberg, E., & Dan, Y. (2010). Contribution of semi-arid forests to the climate system. *Science*, *327*, 451–454. https://doi.org/10.1126/science.1179998

Roxy, M. S., Sumithranand, V. B., & Renuka, G. (2010). Variability of soil moisture and its relationship with surface albedo and soil thermal diffusivity at Astronomical Observatory, Thiruvananthapuram, South Kerala. *Journal of Earth System Science*, *119*(4), 507–517. https://doi.org/10.1007/s12040-010-0038-1

Sellers, P. J., Mintz, Y., Sud, Y. C., & Dalcher, A. (1986). A simple biosphere model (SiB) for use within general circulation models. *Journal of Atmosphere Sciences*, *43*, 505–531.

Shi, G. Y., Hayasaka, T., Ohmura, A., Chen, Z. H., Wang, B., Zhao, J. Q., Che, H. Z., & Xu, L. (2008). Data quality assessment and the long-term trend of ground solar radiation in China. *Journal of Applied Meteorology and Climatology*, *17*, 1006–1016. https://doi.org/10.1175/2007JAMC1493.1

Song, J. (1998). Diurnal asymmetry in surface albedo. *Agricultural and Forest Meteorology*, *92*, 181–189.

Trenberth, K. E., & Fasullo, J. T. (2009). Global warming due to increasing absorbed solar radiation. *Geophysical Research Letters*, *36*, L07706. https://doi.org/10.1029/2009GL037527

Trenberth, K. E., Fasullo, J. T., & Kiehl, J. (2009). Earth's global energy budget. *Bulletin of the American Meteorological Society*, *90*(3), 311–323. https://doi.org/10.1175/2008BAMS2634.1

Tsvetsinskaya, E. A., Schaaf, C. B., Gao, F., & Lucht, W. (2002). Relating MODIS-derived surface albedo to soils and rock types over Northern Africa and the Arabian Peninsula. *Geophysical Research Letters*, *29*(9), 1353. https://doi.org/10.1029/2001GL014096

Wang, C., Wei, Z. G., & Li, Z. C. (2010). A quality control routine for Dunhuang Gobi meteorology tower data [in Chinese with English abstract]. *Journal of Arid Meteorology*, *28*(2), 121–127.

Wang, S., Grant, R. F., Verseghy, D. L., & Black, T. A. (2001). Modelling plant carbon and nitrogen dynamics of a boreal aspen forest in CLASS-the Canadian Land Surface Scheme. *Ecological Modelling*, *142*(1–2), 135–142.

Wang, S., Grant, R. F., Verseghy, D. L., & Black, T. A. (2002a). Modelling carbon dynamics of a boreal forest in ecosystems using the Canadian Land Surface Scheme. *Climatic Change*, *55*(4), 451–477.

Wang, S., Grant, R. F., Verseghy, D. L., & Black, T. A. (2002b). Modelling carbon-coupled energy and water dynamics of a boreal aspen forest in general circulation model Land Surface Scheme. *International Journal of Climatology*, *22*, 1249–1265. https://doi.org/10.1002/joc.776

Wang, Z., Zeng, X., Barlage, M., Dickinson, R. E., Gao, F., & Schaff, C. B. (2004). Using MODIS BRDF and albedo data to evaluate global model land surface albedo. *Journal of Hydrometeorology*, *5*(1), 3–14.

Wei, Z. G., Huang, R. H., & Chen, W. (2006). Transfer coefficients of sensible heat under the atmospheric stability in near surface layer over Dunhuang Gobi [in Chinese with English abstract]. *Plateau Meteorology*, *25*(2), 834–839.

Wen, L. J., Lv, S. H., Chen, S. Q., Meng, X. H., Li, S. S., & Ao, Y. H. (2009). Observation study on diurnal asymmetry in surface albedo of oasis in arid region [in Chinese with English abstract]. *Acta Energiae Solaris Sinica*, *30*(7), 953–956. https://doi.org/0254-0096(2012)11-1937-07

Xue, Y., Sellers, P. J., Kinter, J. L., & Shukla, J. (1991). A simplified biosphere model for global climate studies. *Journal of Climate*, *4*, 345–364.

Xue, Y., & Shukla, J. (1993). The influence of land surface properties on Sahel climate. Part I: Desertification. *Journal of Climate*, *6*, 2232–2245. https://doi.org/10.1175/1520-0442(1993)006<2232:TIOLSP>2.0.CO;2

Xue, Y., Zeng, F. J., & Schlosser, C. A. (1996). SSiB and its sensitivity to soil properties a case study using HAPEX-Mobilhy data. *Global and Planetary Change*, *13*, 183–194.

Zhang, Q., Cao, X. Y., Wei, G. A., & Huang, R. H. (2002a). Observation and study on land surface parameters over Gobi in typical arid region. *Advances in Atmospheric Sciences*, *19*(1), 121–135.

Zhang, Q., & Huang, R. H. (2004a). Water vapor exchange between soil and atmosphere over a Gobi surface near an oasis in summer. *Journal of Applied Meteorology*, *43*, 1917–1928.

Zhang, Q., & Huang, R. H. (2004b). Parameters of land-surface processes for Gobi in North-West China. *Boundary-Layer Meteorology*, *110*(3), 471–478. https://doi.org/10.1023/B:BOUN.0000007224.08804.b8

Zhang, Q., Huang, R. H., Wang, S., Wei, G. A., Cao, X. Y., Hou, X. H., . . . Yan, Y. P. (2005). NWC-ALIEX and its research advances [in Chinese with English abstract]. *Advances in Earth Sciences*, *20*(4), 427–441.

Zhang, Q., Wang, S., & Wei, G. A. (2003). A study on parameterization of local land-surface physical processes on the Gobi of Northwest China [in Chinese with English abstract]. *Chinese Journal of Geophysics*, *46*(5), 616–623. https://doi.org/10.1002/cjg2.408

Zhang, Q., Wei, G. A., & Huang, R. H. (2002b). The study of the atmospheric bulk transfer coefficient over desert and Gobi in arid region of northwestern China [in Chinese with English abstract]. *Science in China, Series D*, *45*(5), 468–480.

Zheng, Z. Y., Dong, W. J., Li, Z. C., Zhao, W., Hu, S. S., Yan, X. D., . . . Wei, Z. G. (2015). Observational study of surface spectral radiation and corresponding albedo over Gobi, desert, and bare loess surfaces in northwestern China. *Journal of Geophysical Research: Atmospheres*, *120*, 883–896. https://doi.org/10.1002/2014JD022516

Zheng, Z. Y., Wei, Z. G., Li, Z. C., & Wang, C. (2012). Characteristics of solar spectral radiation and albedo during early autumn in Dunhuang Gobi [in Chinese with English abstract]. *Acta Energiae Solaris Sinica*, *33*(11), 1937–1943.

Zheng, Z. Y., Wei, Z. G., Li, Z. C., Wei, H., & Liu, H. (2014). Study of parameterization of surface albedo of bare soil over the Gobi Desert in the Dunhuang region [in Chinese with English abstract]. *Chinese Journal of Atmosphere Sciences*, *38*(2), 297–308. https://doi.org/10.3878/j.issn.1006-9895.2013.13147

Zheng, Z. Y., Wei, Z. G., Wen, Z. P., Dong, W. J., Li, Z. C., Wen, X. H., . . . Hu, S. S. (2017). A study of variation characteristics of Gobi broadband emissivity based on field observational experiments in northwestern China. *Theoretical and Applied Climatology*, 1–12. https://doi.org/10.1007/s00704-017-2056-2

Zhou, D. G., & Huang, R. H. (2011). Characterization of turbulent flux transfer over a Gobi surface with quality-controlled observations. *Science China Earth Sciences*, *54*(5), 753–763. https://doi.org/10.1007/s11430-010-4055-3